Optical Fiber Technology 81 (2023) 103541

Contents lists available at ScienceDirect

Optical Fiber Technology

journal homepage: www.elsevier.com/locate/yofte

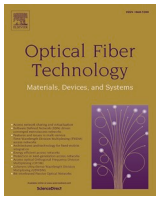

Interconnectivity between effectively single-moded antiresonant hollow core fibres and conventional single-mode fibres

Radan Slavík [a,*], Matěj Komanec [b], Eric Numkam Fokoua [a,c]

[a] Optoelectronics Research Centre, Univeristy of Southampton, Southampton SO7 1BJ, UK
[b] Faculty of Electrical Engineering, Czech Technical University in Prague, Technická 1902/2, 166 27, Czechia
[c] Now with Microsoft Inc., Romsey, UK

ARTICLE INFO

Keywords:
Hollow core optical fibres
Fibre optics
Integration of hollow core fibres in standard fibre systems

ABSTRACT

We review the topic, focusing first on a discussion of the key parameters, limits of coupling loss, and measurement techniques. We then follow by reviewing the literature, including mode-field adaptation methods, and assembly approaches. Finally, we briefly cover the topic of hollow core fibre connection with non-standard single mode fibres, and finish with a review of components that can be made directly within the connection. We conclude with a summary of key achievements and present our view on key remaining challenges.

1. Introduction

Hollow core optical fibres (HCFs) have many unique properties when compared to solid glass-core fibres such as standard silica glass-made single-mode-fibres, SMFs. Although we can expect that future fibre components and subsystems for HCF-based systems would be available with HCF pigtails (i.e., directly connected to HCFs), it is important to ensure the "back-compatibility" with the existing SMF-based systems. Such compatibility is also important to enable a "combination of the best of both technologies" (SMF and HCF) in a single fibre-optic system.

A connection between HCF and SMF has four key performance metrics: coupling loss, coupling modal purity, (parasitic) back-reflection, and stability. In the following analysis, we first discuss how some unique features of HCF need to be considered in evaluation of these four parameters, since these features have not always been given due consideration in published works. Following this, we review methods used to evaluate these parameters, as well as achievable performance, before finishing with reviewing the current state-of-the-art.

2. Interconnection parameters

HCFs are usually not single-moded, as this would require relatively small core diameters that in turn lead to relatively high attenuation (shown, e.g., in Fig. 14 in Ref. [1]). We categorize HCFs into those intended to operate over the fundamental mode only (similarly to SMFs) and those designed to operate over more modes (similarly to few-mode or multi-mode solid glass-core fibres) [2,3]. Here, we will refer to those intended to operate over the fundamental mode only as "effectively single-moded", an expression that we elaborate on in the next paragraph. In this paper, we limit our analysis to coupling between effectively single-moded HCFs and SMFs, with coupling between fibres designed to operate over more modes being outside our scope.

Attenuation of the fundamental mode in HCFs is usually the lowest of all guided modes with higher order modes (HOMs) having higher attenuation [1]. By engineering the fibre structure, the attenuation of the lowest-loss HOM can be significantly enhanced. Thus, any light coupled into HOMs is quickly attenuated (we come back to how "quickly" later), making the fibre "effectively single-moded". It is, however, important to keep in mind that "single-mode" and "effectively single-mode" are not identical and that effectively single-moded HCFs behave as single-moded only under certain assumptions. To evaluate this, two main effects need to be considered. First, it is the coupling modal purity, i.e., how much light at the HCF input is cross-coupled into the HOMs (and/or reciprocally, how much light from the HCF HOMs is cross-coupled into SMF). Secondly, it is how much light launched into the HCF fundamental mode couples into HOMs and then back during the propagation due to fibre imperfections and perturbations. This second property does not depend on the SMF-HCF connection (e.g., it is present even with a perfect fundamental mode launch) and thus is outside the scope of this article.

Today, the lowest-loss effectively single-moded HCFs use antiresonance guidance and a nodeless design, in which (nested) tubes are

* Corresponding author.
E-mail address: r.slavik@soton.ac.uk (R. Slavík).

https://doi.org/10.1016/j.yofte.2023.103541
Received 31 May 2023; Received in revised form 31 August 2023; Accepted 1 October 2023
Available online 11 October 2023

placed around the central hollow core. We will refer to them as "tubular" (single-tubes), Nested Antiresonant Nodeless Fibres "NANFs" (nested tubes) and Double NANFs, "DNANFs" (double-nested tubes), see Fig. 1. In NANFs, the lowest HOM attenuation of up to 2800 dB/km (2.8 dB/m) has been reported [4] for a fibre with fundamental mode attenuation of 0.22 dB/km. However, this lowest HOM lattenuation varies significantly as it is driven by small changes in the geometry of the fibre cross-section. For example, lower values have been reported, e.g., ~100 dB/km for 0.174 dB/km DNANF [5] or as little as 6–12 dB/km in earlier low-loss (e.g., 0.28 dB/km) NANF designs [6].

For an illustration, let us consider two values of the lowest-loss HOM attenuation: 2800 dB/km (highest value reported) and 100 dB/km (value reported for the lowest-loss HCF [5]). Considering fundamental mode attenuation of < 1 dB/km, we can neglect it in the further analysis for simplicity. Let us also consider that we couple 90% of light from SMF into the HCF fundamental mode (coupling loss of ~ 0.5 dB) and 1% into the lowest-loss HOM (cross-coupling of −20 dB). To reach desired extinction ratio of 60 dB [5], we need to propagate it through 15 and 410 m, respectively, for our two examples considered. Consequently, in HCF applications that deal with fibres of this length or shorter, more careful consideration of the single-modeness is required.

Let us consider another important example in which we couple light to and from an HCF with two identical SMFs, Fig. 2. This represents a "pigtailed" HCF with SMFs or an HCF gas cell with SMF pigtails. We consider HCF length of 10 m and input power of 1 mW, of which 0.9 mW is coupled into the HCF fundamental mode and 1% (10 μW) into the LP_{11} (the lowest-loss HOM with attenuation of 100 dB/km). Light propagating in LP_{11} experiences 1 dB of loss, which we neglect in this illustration. As the second HCF-SMF connection is identical to the first one, we couple 0.81 mW of the HCF fundamental mode into the SMF and 1% of LP_{11} (0.01 × 10 μW = 100 nW) is coupled back into the SMF, where these two modes interfere, causing multi-path interference. It may seem that 100 nW from LP_{11} versus 0.81 mW from the fundamental mode (39 dB difference) should produce very small effect. In reality, the situation is different, as we deal with interference in which fields are summed rather than intensities. Mathematically, the power at the output SMF when neglecting propagation loss in the HCF is given by [12]:

$$P_{out} = P_{in}(\alpha^2 + 2\alpha\beta\cos(\omega\tau) + \beta^2) \quad (1)$$

where α is the SMF-HCF fundamental mode coupling loss (0.9 in our example), β is the cross-coupling to the HOM (1% in our example), ω is the carrier frequency, and τ is the differential delay between the two modes accumulated inside the HCF. In our example, it makes the output power to fluctuate by as much as ± 2.5% (±0.1 dB) depending on τ and ± 2.5% power variation in the transmission spectrum [12]. Such power variation is thus relatively significant (despite having only 1% cross-coupling to a HOM) and may need to be considered in many applications.

To illustrate this, we have inserted a 3-m long DNANF between two optimized graded-index-based mode field adapters (we discuss this in detail later). We first aligned the input and output (Fig. 2) usingx, y, z stages, obtaining SMF_{in}-HCF-SMF_{out} transmission loss of 0.90 dB. As this loss includes two SMF-HCF interfaces, it corresponds to 0.45 dB per single SMF-HCF interface. Spectral transmission is shown in Fig. 3. Subsequently, we aligned also the pitch and yaw of both SMF-HCF

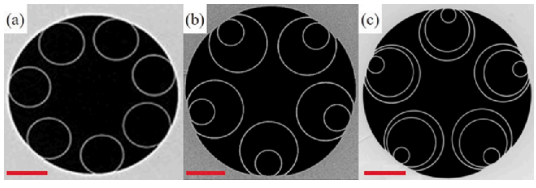

Fig. 1. Scanning electron micrographs of tubular [7], NANF [8], and DNANF [9] fibres' microstructure.

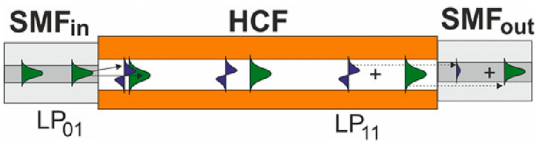

Fig. 2. SMF-HCF-SMF component. At the HCF input, part of the light is cross-coupled into HOMs (LP_{11} shown here for illustration). After accumulating phase/delay difference in respect to the fundamental mode (LP_{01}), part of it is cross-coupled into the output SMF, interfering with the light that propagated in the HCF fundamental mode, causing multi-path interference.

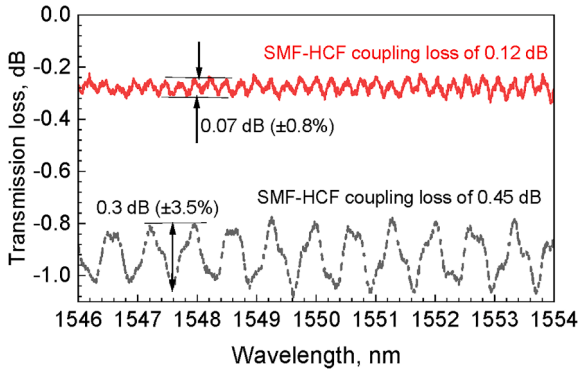

Fig. 3. Measured transmission through a SMF-HCF-SMF with 3-m long DNANF. Black, dashed: both interfaces aligned using x,y,z stages. Red, solid: pitch and yaw on both interfaces has been also aligned. (For interpretation of the references to colour in this figure legend, the reader is referred to the web version of this article.)

interfaces, leading to loss reduction down to 0.26 dB (single SMF-HCF coupling loss of 0.13 dB), its spectral transmission is also in Fig. 3. We can see that the spectral ripples that were ± 3.5% (0.3 dB peak-to-peak) for the 0.45-dB SMF-HCF connection reduced to ± 0.8% for the 0.13-dB SMF-HCF connection. In many applications, such spectral ripples (e.g., gas cells or sensors) may degrade the system performance and thus it is important to consider them.

In terms of parasitic back-reflection, it stems mainly from the Fresnel reflection as the light travels from a glass core (SMF) into the 'empty space' in the HCF core. This is typically 3.5% for silica-air interface, corresponding to −14.5 dB (10log(0.035)) of back-reflection and −0.155 dB of transmission loss (10log(1–0.035)). Angle-cleaved connection is not as straightforward as for, e.g., SMFs connectors, as light refracts at the glass-air interface, increasing coupling loss: we cover this topic in detail later. The key message here is that a "fast wisdom" from dealing with SMFs might be often misleading.

The last parameter to discuss is connection stability. Current HCFs degrade when cleaved and left to open atmosphere [10] and unsurprisingly, there are no reports (to the best of our knowledge) on long-term stability of SMF-HCF connections that have not been sealed.

3. Limits to coupling loss into HCFs

Mode field profiles of different SMFs may differ slightly, but can be approximated by a Gaussian profile for weakly-guided SMFs. In this subsection, we study coupling loss between a free-space Gaussian beam (emulating SMF output) and the fundamental mode of an HCF. Indeed, the real mode-field shape at the HCF input will have some deviations from Gaussian, however, the results shown here demonstrate important trends of the coupling loss with respect to, e.g., input beam size, anti-resonance order, HCF fabrication imperfections, and details of the HCF geometry such as the number of tubes surrounding the core. This analysis is shown in detail in [8], so here, we will only summarize the key results.

Firstly, the coupling loss is minimized when the launch beam width (measured at $1/e^2$ of power intensity profile) is approximately 70% of the HCF core diameter (as defined in Fig. 4) [8]. The minimum value depends on the antiresonance order in which we operate the HCF, e.g., low-loss HCFs designs considered in [8] are predicted to achieve 0.13, 0.07, and 0.09 dB minimum coupling loss for the 1st, 2nd, and 3rd anti-resonance window, respectively. The reason behind the 2nd window performing better than the 1st and 3rd is that the field changes sign in the 1st and 3rd window as it passes through the tubes at the core edges, providing less overlap with the Gaussian mode that does not have any such phase changes in its profile. This is discussed in detail in [8] and [11]. The authors in [8] also concluded that larger number of tubes in the cladding (e.g., 10 instead of 6, as shown in Fig. 1) makes the HCF mode more similar to the circularly-symmetric Gaussian shape, reducing the coupling loss. For the 1st antiresonant window, this decreased coupling loss down to 0.10 dB. Using the same simulation for the 2nd window, we found that the loss can be reduced down to 0.05 dB. However, it is important to point out that such HCF designs may not be optimized for the attenuation or for effective single-modeness.

In terms of HOMs, the LP_{11} usually shows the lowest loss in (D) NANFs. For perfectly symmetric HCF structure and optimized launch, there is no coupling into this mode due to the symmetry. For a realistic (fabricated) structures, the calculated minimum coupling should be around −40 dB [12], which has been in good agreement with experiments where the launch was optimized using all 5 degrees of freedom (x, y, z, pitch, and yaw) [12]. LP_{02} was predicted to get −24 dB coupling [12], which is relatively high. Despite its relatively high loss (e.g., 2100 dB/km in [12]), it may need to be considered when using shorter (<20 m) lengths of an HCF.

4. Coupling loss measurement methods

As mentioned earlier, we focus here on HCFs intended to operate over the fundamental mode only. Before we discuss how to measure the coupling loss (loss between an SMF and the fundamental mode of the HCF), let us show how it should not be measured, despite at first seeming like a reasonable method, Fig. 5. Here, we detect reference signal at the output of the SMF using a photodiode (PD) first. Already here, the first issue arises. We are discarding the Fresnel loss, which for silica SMF is 3.5% (0.155 dB) at the SMF end-face. This power is lost even when using angled end-face, as the SMF is terminated in free space. Second problem arises when measuring transmission through the HCF which is strictly speaking multimoded. A portion of the light is coupled into HOMs and forms part of the detected signal. Both of these mentioned issues lead to a systematic underestimate of the loss. We believe that this is behind some "good values" published, especially in earlier literature.

There are in principle three methods to avoid these problems, as depicted in Fig. 6. The first method is based on using sufficiently long piece of HCF, ensuring all higher-order modes suffer from high loss (e.g., >20 dB, but ideally > 40–60 dB), Fig. 6a. Based on our previous analysis, this may require as little as tens of meters of HCF when an HCF with high HOM attenuation (e.g., >2000 dB/km for the lowest-attenuation HOM) is used. For a typical low-loss HCF reported in the literature (e.g., [6]), however, this may be significantly more, e.g., >100–1000 m. The key is to know the attenuation of HOMs first and ensure sufficiently long HCF sample is used. The second method is in fact a group of methods that are based on HCF modal analysis, Fig. 6b. As they give power carried by each individual mode, they could be used for coupling and cross-coupling analysis into each of these modes at the HCF input. Two examples of these methods are the time of flight [13] and S^2 analysis [14,15], Fig. 6b. Time of flight sends short pulses through the HCF and detects a series of pulses at the output, each of them arriving at slightly different time due to the difference in the group refractive indices of the guided modes. S^2, which stands for "spatially and spectrally resolved imaging" monitors the mode field profile at the output and thanks to scanning the wavelength, enables decomposition of the mode profiles, their effective refractive indices, and mode content with power carried by each considered mode. All the methods above must consider the input Fresnel loss (0.155 dB) correctly to obtain the true coupling loss. Unfortunately, this is often omitted in published results. For monitoring of coupling efficiency and coupling into HOMs using already-characterized/known HCF, a simpler approach can be used. When effective refractive indices of modes and their attenuation are known (at

Fig. 4. Definition of core diameter: diameter of the largest circle that can be drawn inside the central hole.

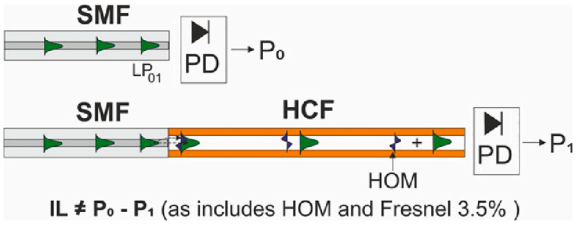

Fig. 5. Incorrect measurement of the coupling loss. P_0 is lower than the signal level in the SMF (by 0.155 dB), as 3.5% typically does not reach the PD due to the Fresnel reflection (present also in an angle-cleaved SMF). Further, P_1 includes also HOMs power, which should be excluded. This leads to underestimation of loss, which is sometimes significant.

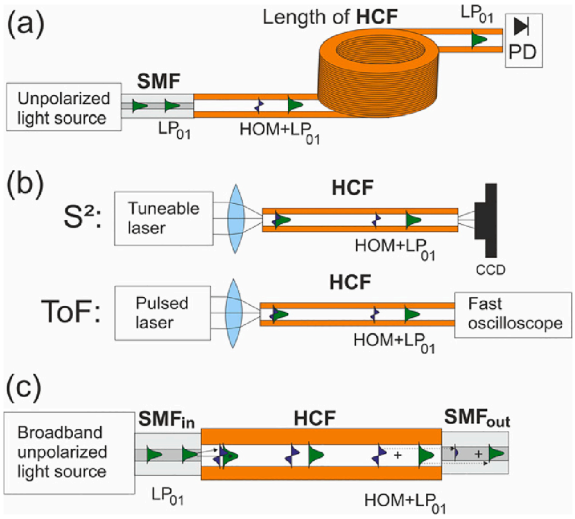

Fig. 6. Three ways to measure coupling loss. (a) Long-enough HCF is used to attenuate all HOMs (may require > 1 km of HCF); (b) S^2 and Time of Flight (ToF) measurements, here shown in configurations to provide HCF modal characterization. As they distinguish between modes, they could be used for coupling and cross-coupling loss measurement; (c) Simple method for HCF-SMF connection characterization using identical coupling into SMF on both sides of the HCF.

least approximately), simple and fast (of interest, e.g., during the alignment) spectral analysis provides useful information about coupling into HCF modes, Fig. 6c [12]. Besides its speed, its further advantage is that it only needs measurement devices widely available in fibre-optics labs (e.g., erbium doped fibre amplifier, EDFA used as an unpolarized broadband light source, and Optical Spectrum Analyzer, OSA). Further, it needs only relatively short lengths of HCF, typically up to 20 m. Its slight disadvantage is that it needs to connect the HCF to identical SMF on both sides. We find this method particularly useful for evaluation of HCF-SMF connection, which is why we review it more in detail in the following text.

The setup for measuring HOM content in Fig. 6c is identical to schematics we analyzed in Fig. 2, where Eq. (1) describes the modal interference at the output. However, it neglects the propagation loss. This can be neglected for the fundamental mode for relatively short (<50 m) low-loss (<1 dB/km) HCFs. However, HOM loss usually cannot be neglected, changing Eq. (1) into:

$$P_{out} = P_{in}(\alpha^2 + 2\alpha\beta\sqrt{\gamma}\cos(\tau) + \gamma\beta^2) \quad (2)$$

where γ is the HOM power propagation loss. The square root is present as we deal with the field rather than intensities at the subsequent observation of multipath interference.

To simplify our further analysis, we will neglect the coupling loss of the fundamental mode (α = 1). Further, we neglect the second order term β^2, as β is typically small (e.g., 0.01 in our previous examples). These assumptions simplify Eq. (2) to:

$$P_{out} = P_{in}\left(1 + 2\beta\sqrt{\gamma}\cos(\omega\tau)\right). \quad (3)$$

Then, the Fourier transform of the measured normalized transmission is [12]:

$$\mathcal{F}\left(1 + 2\beta\sqrt{\gamma}\cos(\omega\tau)\right) = \delta(t) + \beta\sqrt{\gamma}\delta(t-\tau). \quad (4)$$

The term $\delta(t)$ describes the arrival of the signal propagating within the HCF fundamental mode, while the term $\beta\sqrt{\gamma}\delta(t-\tau)$ describes beating between light propagating in the HCF fundamental mode and the particular HOM. For illustration, we show in Fig. 7 Fourier transform of the measured data shown in Fig. 3. We observe two prominent peaks corresponding to fundamental mode beating with LP_{11} and LP_{02} modes, which appear at delays expected from the HCF length (3 m) and HCF numerical analysis (predicting delay of 3 and 8 ps/m, respectively [12]). Amplitude of these peaks depends on both, the HOM cross-coupling β and HOM loss γ, Eq. (4). By knowing HOM attenuation (e.g., from simulations), coupling coefficient β can be found. Another option is to prepare two samples of different lengths, for which the coupling coefficient β would be identical, but HOM loss γ will scale with the HCF length.

Fig. 7 shows that cross-coupling into LP_{11} was strongly suppressed when aligning the pitch and yaw, which also reduced the insertion loss (from 0.45 to 0.13 dB for SMF-HCF interface). In this particular example, it is below −32 dB, most likely caused by limited symmetry of the fabricated HCF [12]. As for the LP_{02}, we see cross-coupling at −26 dB level, however, considering typical attenuation of LP_{02} in DNANFs of 2 dB/m, the coupling into this mode (Eq. (4)) is expected to be around −23 dB. As we see in this particular example, Fig. 7, the power variation shown in Fig. 3 is mostly limited by LP_{02} when pitch/yaw are well aligned and by LP_{11} when they are not fully optimized. The above analysis is an example of how the HCF-SMF interconnection can be analyzed, troubleshooted, and ultimate performance found.

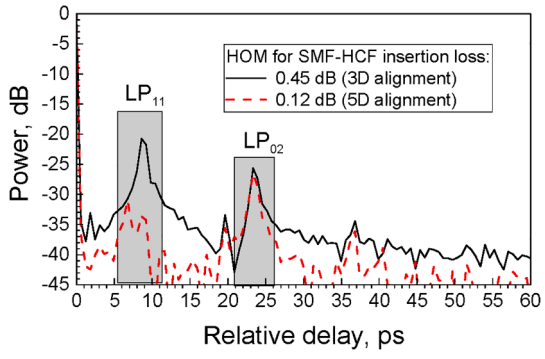

Fig. 7. Fourier transform of transmission spectra shown in Fig. 3, showing peaks corresponding to fundamental mode beating with the LP_{11} and LP_{02} modes.

5. Mode-field diameter adaptation methods

As mentioned earlier, lowest coupling loss is obtained with input beam with mode size (characterized by the mode field diameter, MFD) about 70% of the low-loss HCF core diameter. Recently reported low-loss HCFs typically have core diameters between 20 and 40 μm, corresponding to the optimum launch MFD of 14 –28 μm. The most straightforward approach is to use an SMF with matching MFD, e.g., Large Mode Area (LMA) fibre used in high power applications [16]. For example, a tubular HCF was spliced to an MFD-optimized LMA using this approach [16]. However, in most applications, the SMF mode would have different MFD to that of the HCF, which requires an MFD adaptation method.

Various mode field adaptation methods have been reported, especially to adapt the MFD of the standard telecom SMF (MFD ~ 10 μm at 1550 nm) to that of the used HCF. Use of micro lenses [17], thermally-expanded core (TEC) [12], inverse taper [18], taper [19], and graded index (GRIN) lens/fibres [12] have been reported, see Fig. 8. We do not cite here achieved coupling loss, as some of them consider solely coupling into the HCF fundamental mode, while others do not (often facing one of the characterization pitfalls mentioned earlier). However,

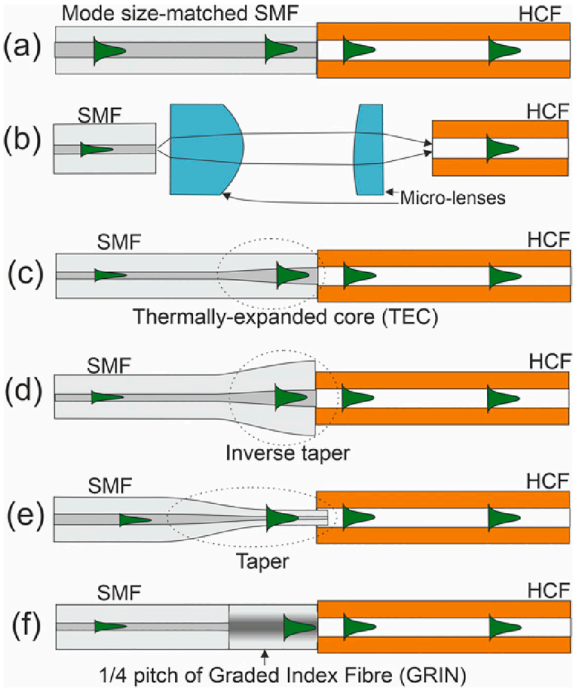

Fig. 8. Methods to adapt mode field diameter between SMF and HCF. (a) SMF with mode field diameter matched to HCF is used [16]; (b) A pair of micro-lenses is used [17]; (c) Thermally-expanded core (TEC) [12]; (d) Inverse taper [18]; (e) Taper inserted into the HCF hollow core [19], (f) a short segment (1/4 pitch length) of a graded index fibre (GRIN) serves as a GRIN lens with focal point at its output.

we expect that all these methods should be able to achieve coupling close to that predicted theoretically from a Gaussian mode provided the light is not lost in back-reflection due to the Fresnel loss (0.155 dB). The lowest numbers reported are below 0.2 dB, which is sufficiently-low for most applications and comparable to a fibre-optic connector connection between SMFs or splice loss between dissimilar SMFs.

As for HOM parasitic cross-coupling, only limited information is provided in the literature, with values below −35 dB for LP_{11} and below −21 dB for LP_{02} reported, e.g., in [12]. Recently, lower-loss LP_{02} coupling (<-35 dB) has been achieved [22] when optimizing SMF-HCF coupling loss (measured 0.079 ± 0.006 dB vs 0.0074 dB minimum simulated). We believe such low coupling into HOMs is of significant importance for applications sensitive to multipath interference.

6. Connection methods

The connection can be permanent or detachable. Spliced or glued connections are typical examples of a permanent connection. Optical connectors that can be assembled and disassembled many times represent a detachable connections. In the literature, there are examples of a "connector style" HCF-SMF connections, but they generally refer to the fact that some of the equipment used in connectors is employed and may, for example, require HCF cleave every time prior to assembly. The key question with these connections is how they manage the HCF end-face degradation due to access of atmospheric air (e.g., moisture reported to degrade the performance [10]). In the following analysis, we do not discuss reported HCF-SMF connections that are reasonably expected to degrade without further modifications (e.g., via sealing).

Permanent connection can be glued or spliced. The advantage of the glued connections is the possibility of introducing a gap [20], AR coating, and to angle-cleave/polish SMF while keeping HCF flat-cleaved [12]. Spliced connections on the other hand are expected to withstand larger range of temperatures, chemically-aggressive environments, and high pressures.

Detachable connections should consist of an HCF with protected (sealed) end-face, preventing degradation and enabling its cleaning. Subsequently, it should operate as standard fibre connectors, as e.g., in [21].

6.1. Permanent connections via splicing

Fusion splicing is very popular connection approach, as it allows to use a range of advanced splicers developed for optical fibres, using arc, filament, or CO_2 laser for heating. When splicing an SMF with suitable mode field adaptation (as discussed earlier) with an HCF, parameters should be optimized to avoid collapse or deformation of the HCF inner microstructure. The key disadvantage is the Fresnel 3.5% reflection, which especially in "'pigtailed HCF" configuration (as shown in Fig. 2) is problematic, as it creates parasitic Fabry-Perot resonances, responsible for up to ± 7% transmission power fluctuations [23]. There has been a recent report using an AR coating deposited on the SMF [24] with back-reflection reduced to −28 dB. This should lead to a significant reduction of parasitic Fabry-Perot etalon power variations (down to ± 0.3%). It is challenging, however, to predict how this promising technique could be further improved for applications that require lower back-reflection such as Optical Time Domain Reflectometry of HCFs [25] that requires back-reflection below −40 dB or how stable it is with time. These concerns arise because the coating was reported to degrade during the fusion splicing [24] and available literature [26] suggests that such degradation is expected already above 400°C (and below 1000°C), which is well-below the temperature needed for mechanically-strong fusion splicing.

Another approach is to splice angle-cleaved SMF and HCF, Fig. 9. This does not avoid loss due to the 3.5% Fresnel reflection, but this reflected light is not back-reflected thanks to the angled cleave, Fig. 9a. Besides reflection loss, another drawback of this configuration is that

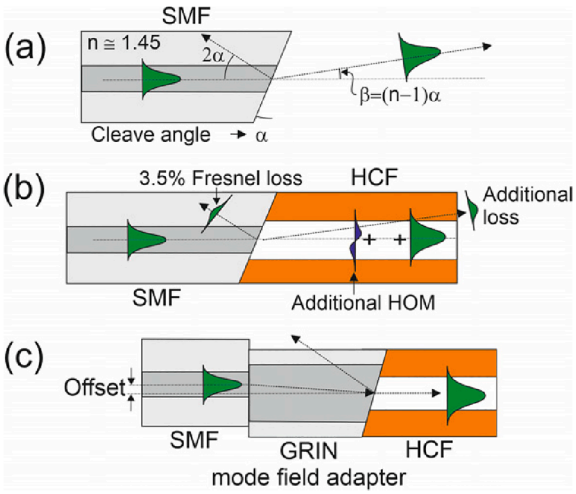

Fig. 9. Angle-cleaved connections for splicing (mode field adapter not shown in (a) and (b) for simplicity). (a) Light leaves an angle-cleaved SMF under an angle β. There is also a Fresnel reflection, which is only weakly-coupled back (producing weak back-reflection), but this power is lost, reducing power at the SMF output. (b) In angle-cleaved SMF spliced with HCF, part of light is coupled into radiation modes (causing additional loss) and part into HOMs due to the angle β. A compromise between reduced back-reflection and increased coupling loss can be found [27]. (c) Such trade-off is avoided when using GRIN mode field adapter in which SMF is spiced with an offset to the GRIN, generated collinear beam at the output, enabling both, low loss and low back-reflection [28].

light refracts at the SMF surface under an angle, Fig. 9b, reducing coupling efficiency into the HCF and increasing HOM excitation. In [27], authors studied the trade-off between the back-reflection suppression and transmission loss as a function of the cleave angle. They found and demonstrated that 1 and 2° angles reduced the back-reflection to −25 and −40 dB when increasing the coupling loss only moderately to 0.85 and 1.25 dB, respectively.

Recently, it was suggested how to avoid the trade-off between the cleave angle and coupling loss by applying offset splicing of the SMF to the GRIN mode field adapter, Fig. 9c [28]. The coupling loss of unspliced coupling into a flat-cleaved HCF was measured to be 0.85 dB with back-reflection below −50 dB. Although this shows the proof-of-principle, demonstration of this technique will require angle-cleaving of HCF and splicing, which has not been demonstrated yet. However, simulations promise back-reflection below −60 dB with coupling loss below 0.5 dB.

6.2. Permanent connections via gluing

Although gluing is not a usual technique to connect optical fibres together, it has been well established for fibre pigtailing of various waveguide platforms such as $LiNbO_3$ modulators or NxN power splitters and couplers. As it is a "cold" process, it enables application of AR coatings [12], achieving back-reflection of −40 dB over 50 nm bandwidth [12] while achieving low coupling loss of 0.15 dB. This low level is partially achieved thanks to no deformation of the HCF microstructure that is not heated during the connection process. There is, however, another very important advantage to gluing. It does not require the SMF and HCF to be in a physical contact, Fig. 10a, as glue can "fill the gap". Firstly, this enables alignment in all five degrees of freedom (x, y, z, pitch, and yaw) prior to gluing, making it possible to achieve minimum loss, e.g., 0.15 dB in [12]. It also allows for using an angle-cleaved SMF with HCF flat-cleaved [23] with or without an AR coating [23], Fig. 10b and c. Angle-cleaved SMF enables low back-reflection over a broad spectral range (e.g., 400 nm in [23]), while AR coating further lowers the back-reflection and lowers the coupling loss (by 0.155 dB) by

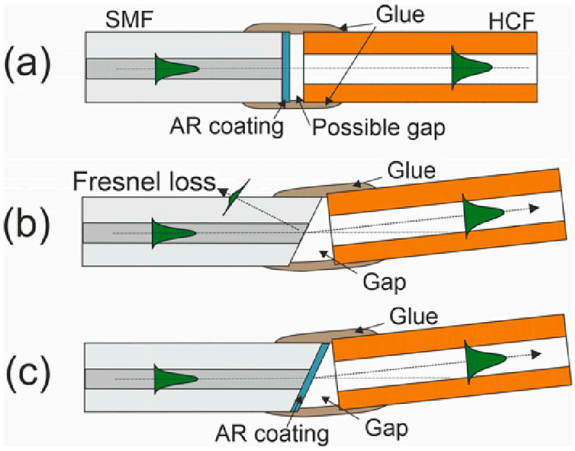

Fig. 10. Glued SMF-HCF connections (mode field adapters and capillaries into which the fibres are in practice glued in, e.g., [12,22,23] are not shown for simplicity). (a) Gluing enables application of AR coating and also introduction of a small gap, enabling accurate alignment including angle. (b) Angle-cleaved SMF can be low-loss aligned to a flat-cleaved HCF and thanks to the gap, glued together. (c) Combining SMF angle-cleaving and AR coating, coupling loss is reduced (as reflection suppressed), back-reflection lowered (a combination effect of the angle and coating), and subsequently smaller cleave angle is required than in (b) to achieve back-reflection below −60 dB. Small angle produces smaller gap, which is also easier to glue.

eliminating the Fresnel loss. Achieved results with this technology are summarized in Table 1. It suggests that the best configuration is AR-coated angle-cleaved SMF. It requires the angle to be only 2°, which is small-enough angle to be glued similarly to the flat configuration. Recently, it was shown that the existence of the gap between the SMF and HCF can be further exploited to obtain even lower coupling loss [20]. It is the first report on experimentally achieving coupling loss at the minimum level predicted by simulations. Specifically, coupling loss of (0.079 ± 0.006) dB was reported for predicted minimum loss of 0.074 dB. This approach is to be verified on angled connection, but so far seems very promising.

In terms of excess loss, the gluing process does not appear to add further loss (with measurement limited by the measurement accuracy to 0.005 dB per SMF-HCF connection) [12,20].

Another class of glued connections are those using microlenses, where fibres are glued with microlenses into a hermetically-sealed package [17] (schematically shown in Fig. 8b). The key advantage of this configuration is the ability to insert functional elements and to make devices with more than one input and output fibres.

6.3. Connector connection

One of the possible approaches is a spliced connection in the "splice-on-connector" fashion in which a pre-cleaved short piece of an SMF glued and polished in a ferule is spliced with the HCF with a suitable mode filed adapter attached to it [29]. This concept can be modified to include the SMF-to-HCF connection directly inside the ferrule, as we suggest in Fig. 11. Realization of this approach, to the best of our knowledge, has not been reported in literature yet.

As for the existing literature, we are aware only of one report that

Table 1
Parameters of glued HCF-SMF connections.

SMF-HCF	Angle, deg	Loss, dB	Back-reflection, dB	Ref.
Flat SMF + AR coating	0	0.15	−40 (over 50 nm)	[12]
		0.079		[20]
Angle SMF	8	0.42	<-60	[23]
Angle SMF + AR coating	2	0.17	<-60 (over 400 nm)	[23]

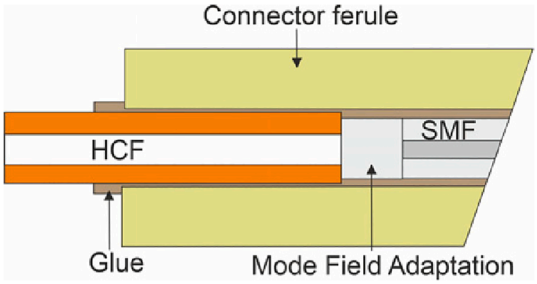

Fig. 11. Possible configuration of a connector with HCF that could be matted to a standard SMF APC connector. The mode field adapter can be almost any of the previously suggested, glued or spliced.

promises stable operation (as mentioned earlier, we do not review approaches than need further engineering to become stable), however, it connects two HCFs [21] rather than SMF with HCF. But we presume it could be modified to enable connection between an SMF and HCF provided SMF has suitable mode field adapter attached to it.

7. HCF connected to specialty fibres

Polarization-maintaining (PM) HCFs have been reported, including their interconnection with a PM SMF [29]. In essence, most connection techniques could be adopted for this, using PM SMF and attach a mode field adapter that does not necessarily need to be PM. This could work provided the mode field adapter is short, e.g., TEC (several mm) [29], or GRIN (100s of μm) and straight.

Other reports included HCF connection with dispersion compensating fibres (DCF) [30] or large-mode-area fibres (LMA) [16]. These were for applications such as short pulse laser delivery where a short segment of a DCF compensates for the low dispersion in the HCF or high-power delivery, where LMA ensures reduced nonlinearity.

8. Components incorporating HCF-SMF connection

Glued HCF-SMF connections have been shown to allow for additional functionalities. Indeed, by replacing the AR coating with a high-reflective coating, a high-Q factor alignment-free Fabry-Perot etalon has been demonstrated [31]. The resonator mirrors were made by thin film filters (similarly to AR coating) and the same technology could be used to deposit other thin-film filters such as gain flattening filters, band-pass, or band-stop filters, of interest, e.g., in Raman spectroscopy, where a strong pump must be filtered out.

To enable insertion of various functional elements, the low-loss HCF-SMF glued connection gap distance has been optimized in [32], showing 200 μm gap and predicting up to 3.7 mm gap using commercially-available graded index fibres as mode field adapters.

The gap could be also used for access to the HCF core by leaving a small hole on the glued connection side [33], of interest for gas sensing and as gas cells [34].

Even more flexible, although more complex is glued solution using microlenses [17]. Its key advantage is the ability to get more than one input and output fibre, enabling 3-port or 4-port devices such as add/drop multiplexers or pump combiners.

9. Conclusions

Connecting hollow core fibres with standard single-mode glass-core fibres is maturing, offering low loss (below 0.2 dB), low back-reflection (below −60 dB) and reasonable mode purity (higher order mode suppression > 20 dB). Although modern low-loss HCFs are effectively single-moded (with all higher order modes lossy), care must be taken when dealing with short (typically 10s to 100s of meters) fibres, which is a length relevant for many applications. Future work will most probably

focus on simplifying the manufacturing process of HCF-SMF connection, possibly making it as straightforward as splicing two dissimilar solid-core fibres today. The greatest challenge is in our view keeping the unwanted cross-coupling to higher order modes low enough for specific applications.

Declaration of Competing Interest

The authors declare that they have no known competing financial interests or personal relationships that could have appeared to influence the work reported in this paper.

Data availability

No data was used for the research described in the article.

Acknowledgements

This work was supported by the Royal Academy of Engineering (RCSFR1718\6\15), the Engineering and Physical Sciences Research Council (EPSRC) under Grants EP/P030181/1 and EP/W037440/1 and the Czech Science Foundation (GACR) grant GA22-32180

References

[1] E. Numkam Fokoua, S.A. Mousavi, G.T. Jasion, D.J. Richardosn, F. Poletti, Loss in hollow-core optical fibers: mechanisms, scaling rules, and limits, Adv. Opt. Photon. 15 (1) (2023) 1–85.

[2] W. Shere, E. Numkam Fokoua, G.T. Jasion, F. Poletti, Designing muti-mode anti-resonant hollow-core fibers for industrial laser power delivery, Opt. Express 30 (22) (2022) 4025–40440.

[3] B. Winter, T.A. Birks, and W.J. Wadsworth, Multimode Hollow-Core Anti-Resonant Optical Fibres, in Frontiers in Optics + Laser Science APS/DLS (Optical Society of America, 2019), paper JTu4A.18.

[4] H. Sakr, T.D. Bradley, G.T. Jasion, E. Numkam Fokoua, S.R. Sandoghchi, I. A. Davidson, A. Taranta, G. Guerra, W. Shere, Y. Chen, J.R. Hayes, D.J. Richardson, F. Poletti, Hollow core NANFs with five nested tubes and record low loss, in: Optical Fiber Communications Conference and Exhibition (OFC), 2021, p. F3A.4..

[5] G.T. Jasion, H. Sakr, J.R. Hayes, S.R. Sandoghchi, L. Hooper, E. Numkam Fokoua, A. Saljoghei, H.C. Mulvad, M. Alonso, A. Taranta, T.D. Bradley, I.A. Davidson, Y. Chen, D.J. Richardson, F. Poletti, 0.174 dB/km hollow core Double Nested Antiresonant Nodeless Fiber (DNANF), in: Optical Fiber Communications Conference and Exhibition (OFC), 2022, p. Th4C.7..

[6] G. Jasion, T.D. Bradley, K. Harrington, H. Sakr, Y. Chen, E. Numkam Fokoua, I. A. Davidson, A. Taranta, J.R. Hayes, D.J. Richardson, F. Poletti, Hollow core NANF with 0.28 dB/km attenuation in the C and L bands, in: In Optical Fiber Communication Conference and Exhimition (OFC), 2022, p. Th4B.4..

[7] Z. Liu, B. Karanov, L. Galdino, J.R. Hayes, D. Lavery, K. Clark, K. Shi, D.J. Elson, B. C. Thomsen, M.N. Petrovich, D.J. Richardson, F. Poletti, R. Slavík, P. Bayvel, Nonlinearity-free coherent transmission in hollow-core antiresonant fiber, J. Lightwave Technol. 37 (3) (2019) 909–916.

[8] V. Zuba, H.C.H. Mulvad, R. Slavík, H. Sakr, F. Poletti, D.J. Richardson, E. Numkam Fokoua, Limits of coupling efficiency into hollow-core antiresonant fibres, J. of Lightwave Technol. (2023). https://ieeexplore.ieee.org/document/10132561.

[9] G.T. Jasion, H. Sakr, J.R. Hayes, S.R. Sandoghchi, L. Hooper, E. Numkam Fokoua, A. Saljoghei, H.C. Mulvad, M. Alonso, A.A. Taranta, T.D. Bradley, I.A. Davidson, Y. Chen, D.J. Richardson, and F. Poletti, 0.174 dB/km Hollow Core Double Nested Antiresonant Nodeless Fiber (DNANF), in 2022 Optical Fiber Communications Conference and Exhibition (OFC), Mar. 2022, pp. 1–3.

[10] S. Rikimi, Y. Chen, M.C. Partridge, T.D. Bradley, I.A. Davidson, A.A. Taranta, F. Poletti, M.N. Petrovich, D.J. Richardson, and N.V. Wheeler, Growth of ammonium chloride on cleaved end-facets of hollow core fibers, Conference on Lasers and Electro-Optics (CLEO) (2020), SF2P.4.

[11] E. Numkam Fokoua, R. Slavík, D.J. Richardson, and F. Poletti, Limits of coupling efficiency into hollow-core antiresonant fibers, Conference on Lasers and Electro-Optics (CLEO) (2021), Stu1Q.4.

[12] D. Suslov, M. Komanec, E. Numkam Fokoua, D. Dousek, A. Zhong, S. Zvánovec, T. D. Bradley, F. Poletti, D.J. Richardson, R. Slavík, Low loss and high performance interconnection between standard single-mode fiber and antiresoannt hollow-core fiber, Sci. Rep. 11 (2021) 8799.

[13] F. Poletti, N.V. Wheeler, M.N. Petrovich, N. Badella, E. Numkam Fokoua, J. R. Hayes, D.R. Gray, Z. Li, R. Slavík, D.J. Richardson, Towards high-capacity fibre-optic communications at the speed of light in vacuum, Nature Photon. 7 (2013) 279–284.

[14] J.W. Nicholson, A.D. Yablon, S. Ramachandran, S. Ghalmi, Spatially and spectrally resolved imaging of modal content in large-mode-area fibers, Opt. Express 16 (10) (2008) 7233–7243.

[15] A. Van Newkirk, J.E. Antonio-Lpez, J. Anderson, R. Alvarez-Aguirre, Z.S. Eznaveh, G. Lopez-Galmiche, R. Amezcua-Correa, A. Schülzgen, Modal analysis of antiresonant hollow core fibers using S2 imaging, Opt. Lett. 41 (14) (2016) 3277–3280.

[16] C. Goel, H. Li, M.R. Abu Hasan, W. Chang, S. Yoo, Anti-resonant hollow-core fiber fusion spliced to laser gain fiber for high-power beam delivery, Opt. Lett. 46 (17) (2021) 4374–4377.

[17] Y. Jung, H. Kim, Y. Chen, T.D. Bradley, I.A. Davidson, J.R. Hayes, G. Jasion, H. Sakr, S. Rikimi, F. Poletti, D.J. Richardson, Compact micro-optic based components for hollow core fibers, Opt. Express 28 (7) (2020) 1518–1525.

[18] C. Wang, R. Yu, B. Bebord, F. Gérôme, F. Benabid, K.S. Chiang, L., Xiao, Ultra-low fusion splicing between negative curvature hollow-core fibers and conventional SMFs with a reverse-tapering method, Opt. Expres 29 (14 (2021) 22470–22478.

[19] W. Huang, Y. Cui, X. Li, Z. Zhou, Z. Li, M. Wang, X. Xi, Z. Chen, Z. Wang, Low-loss coupling from single-mode solid-core fibers to anti-resoannt hollow-core fibers by fiber tapering technique, Opt. Express 27 (26) (2019) 37111–37121.

[20] A. Zhong, M. Ding, D. Dousek, D. Suslov, S. Zvánovec, F. Poletti, D.J. Richardson, R. Slavík, M. Komanec, Gap design to enable functionalities into nested antiresoannt nodeless fiber based systems, Opt. Express 31 (9) (2023) 15035–15044.

[21] R. Nagase, H. Kamitsuna, R. Sasaki, and T. Maejima, Hollow-core fiber connector, 26th Optoelectronics and Communications Conference (OECC) (2021), S4E.3.

[22] A. Zhong, E. Numkam Fokoua, M. Ding, D. Dousek, D. Suslov, S. Zvánovec, F. Poletti, R. Slavík, M. Komanec, Hollow-core to standard single-mode fiber connection with perfect mode-field size adaptation, under review in, J. Lightwave Technol. (2023).

[23] D. Suslov, E. Numkam Fokoua, D. Dousek, A. Zhong, S.S. Zvánovec, T.D. Bradley, F. Poletti, D.J. Richardson, M. Komanec, R. Slavík, Low loss and broadband low back-reflection interconnection between a hollow-core and standard single-mode fiber, Opt. Express 30 (20) (2022) 37006–37014.

[24] C. Wang, R. Yu, C. Xiong, J. Zhu, L. Xiao, Ultralow-loss fusion splicing between antiresonant hollow-core fibers and antireflection-coated SMFs with low return loss, Opt. Lett. 48 (5) (2023) 1120–1123.

[25] R. Slavík, E.R. Numkam Fokoua, T.D. Bradley, A.A. Taranta, M. Komanec, S. Zvánovec, V. Michaud-Belleau, F. Poletti, D.J. Richardson, Optical time domain backscattering of antiresonant hollow core fibers, Opt. Exp. 30 (17) (2022) 31310–31321.

[26] P. Shang, S. Xiong, L. Li, D. Tian, W. Ai, Investigation on thermal stability of Ta_2O_5, TiO_2 and Al_2O_3 coatings for application at high temperature, Appl. Surf. Science 285P (2013) 713–720.

[27] C. Zhang, E. Numkam Fokoua, S. Fu, M. Ding, F. Poletti, D.J. Richardson, R. Slavík, Angle-spliced SMF to hollow core fiber connection with optimized back-reflection and insertion loss, J. of Lightwave Technol. 40 (19) (2022) 6474–6479.

[28] B. Shi, C. Zhang, E.R. Numkam Fokoua, F. Poletti, D.J. Richardson, and R. Slavík, Towards spliced SMF to hollow core fiber connection with low and loss and low back-reflection, Conference on Lasers and Electro-Optics (CLEO), San Diego, CA, May 2023.

[29] M. Corrado, T. Kremp, B. Mangan, K.B. Bradley, Y. Liang, B. Savran, and T. Stafford, Optical connector assemblies for low latency patchcords, Patent WO/2021/127032, 2021.

[30] Z. Zhang, Y. Hong, Y. Sheng, A. Jia, X. Liu, S. Gao, W. Ding, Y. Wang, High extinction ratio nad low backreflection polarization maintaining hollow-core to solid-core fiber interconnection, Opt. Lett. 47 (13) (2022) 3199–3202.

[31] A. Zhong, R. Slavík, D. Dousek, D. Suslov, S. Zvánovec, F. Poletti, D.J. Richardson, and M. Komanec, Direct and low-loss connection between a hollow-core optical fiber and a dispersion compensating fiber for dispersion-free delivery of short optical pulses in hollow-core fiber, Proc. SPIE 12414, High-Power Laser Materials Processing: Applications, Diagnostics, and Systems XII, 1241404 (15 March 2023); doi: 10.1117/12.2648720.

[32] M. Ding, M. Komanec, D. Suslov, D. Dousek, S. Zvánovec, E.R. Numkam Fokoua, T. D. Bradley, F. Poletti, D.J. Richardson, R. Slavík, Long-length and thermally stable high-finesse Fabry-Perot interferometers made of hollow core optical fiber, J. Lightwave Technol. 38 (8) (2020) 2423–2427.

[33] A. Zhong, M. Ding, D. Dousek, D. Suslov, S. Zvánovec, F. Poletti, D.J. Richardson, R. Slavík, M. Komanec, Gap design to enable functionalities into nested antiresonant nodeless fiber based systems, Opt. Exp. 31 (9) (2023) 15035–15044.

[34] D. Suslov, T.W. Kelly, S. Rikimi, A. Zhong, A. Taranta, S. Zvánovec, F. Poletti, D. J. Richardson, M. Komanec, N. Wheeler, R. Slavík, Towards compact hollow-core fiber gas cell. Conference on Lasers and Electro-Optics (CLEO), Paper SW4K.2, 2022.